Journal of Molecular Liquids 227 (2017) 303–308

Contents lists available at ScienceDirect

Journal of Molecular Liquids

journal homepage: www.elsevier.com/locate/molliq

Uptake of Ni(II) from aqueous solution onto graphene oxide: Investigated by batch and modeling techniques

Peng Li [a,b], Huiyi Gao [c,*], Yiquan Wang [a,*]

[a] College of Natural Resources and Environment, Northwest A&F University, 712100 Yangling, PR China
[b] Guidance Center for the Development of "One Village One Brand" Campaign of Shaanxi Province, Xi'an 710003, PR China
[c] Institute of Intelligent Machines, Chinese Academy of Sciences, Hefei 230031, PR China

ARTICLE INFO

Article history:
Received 23 November 2016
Received in revised form 9 December 2016
Accepted 10 December 2016
Available online 14 December 2016

Keywords:
Graphene oxide
Ni(II)
Uptake
Surface complexation modeling

ABSTRACT

The contamination of Ni(II) on the apple orchards soil is more serious nowadays. The uptake of Ni(II) from aqueous solutions on graphene oxide (GO) was investigated by batch, XPS and modeling techniques. The batch experiments indicated that the uptake of Ni(II) on GO increased significantly with increasing pH from 2.0 to 6.0, and the high-level uptake of Ni(II) was observed at pH > 6.0. No effect of ionic strength on Ni(II) uptake indicated inner-sphere surface complexation dominated the uptake of Ni(II) on GO. The maximum uptake capacity of GO for Ni(II) calculated from Langmuir model was calculated to be 81.97 mg/g at pH 5.0 and 293 K. The results of XPS spectra indicated that a variety of oxygen-containing functional groups were responsible for the uptake of Ni(II) on GO. The uptake process of Ni(II) on GO can be satisfactorily fitted by surface complexation modeling using diffuse layer model with two inner-surface complexes. These findings are crucial for the potential application of graphene oxide in the uptake of heavy metals in environmental cleanup.

© 2016 Elsevier B.V. All rights reserved.

1. Introduction

The anthropogenic activities (i.e., tanneries, smelters and sewage sludge application) could be lead to the contamination of Ni(II) in soils [1]. Accumulation of excessive amounts of Ni(II) in soil could lead to the toxic effect on soil plants and/or organisms [2]. Many researchers studied the uptake of Ni(II) on various adsorbents such as clay minerals [3–10] and metal (hydr)oxides [11–16]. In these studies, it is found that the uptake of Ni(II) on various adsorbents decreased with increasing ionic strength. However, the limited uptake capacities of these natural adsorbents could be blocked their practical application for the decontamination of heavy metals from aqueous solutions in environmental cleanup.

Owing to large specific surface area, high chemical reactivity and various oxygenated functional groups, graphene oxide (GO) has been extensively regarded as suitable materials for uptake of heavy metal ions [17–24]. Zhao et al. demonstrated that the maximum uptake capacities of GO on Cd(II) and Co(II) were ~106 and 68 mg/g at pH ~ 6.0 and $T = 303$ K, respectively [25]. The accuracy in modeling of uptake behavior is crucial for the design of uptake treatment units. Ding et al. used extended X-ray absorption fine structure spectra to demonstrate the specific adsorption between Ni(II) and carbon nanofibers [26]. To the authors' knowledge, few studies on the uptake mechanism of Ni(II) on GO by modeling technique was still available nowadays [27–31].

In recent years, surface complexation modeling has extensively been employed to fit the uptake behaviors at the solid-water interface extensively [32–35]. Sun et al. studied the uptake of U(VI) on GO using surface complexation modeling and found that uptake behaviors can be satisfactorily fitted by two inner-sphere surface complexes [36]. A thorough understanding of the uptake behavior of metals at the water-solid interface is therefore of fundamental importance. However, the uptake of Ni(II) on GO by using surface complexation modeling are still scarcely.

The aims of this study are (1) to synthesize GO and characterize the nanostructure and surface properties of GO by using scanning electron microscopy (SEM), transmission electron microscopy (TEM), X-ray photoelectron spectroscopy (XPS) and Fourier transformed infrared spectroscopy (FT-IR); (2) to elucidate the effects of water chemistry, including pH, ionic strength, initial Ni(II) concentrations and temperature, on the uptake of Ni(II) on GO by batch technique; (3) to demonstrate the uptake mechanism of Ni(II) on GO by using surface complexation modeling. This study gives an insight into the removal of heavy metals from large volumes of aqueous solutions in environmental cleanup.

2. Materials and methods

2.1. Materials

Graphite (>200 mesh) was purchased from Tianda Co. Ltd. (Qingdao, China). All reagents (e.g., $KMnO_4$, H_2SO_4 and H_2O_2) of analytical grade were obtained from Sinopharm Chemical Reagent Co., Ltd. The

* Corresponding authors.
E-mail addresses: 0550-6732966@163.com (H. Gao), soilphysics@163.com (Y. Wang).

http://dx.doi.org/10.1016/j.molliq.2016.12.045
0167-7322/© 2016 Elsevier B.V. All rights reserved.

stock solution of Ni(II) was prepared by dissolving $NiNO_3$ (spectroscopic purity, Sigma-Aldrich) into deionized water.

2.2. Synthesis and characterization of GO

The GO was synthesized by the oxidation of graphite under concentration H_2SO_4 solution conditions according to the modified Hummers method [37]. Briefly, flake graphite and $KMnO_4$ solid were added into concentrated H_2SO_4 under the ultrasonication conditions for 5 days, then H_2O_2 was added to eliminate the excess MnO_4^- anions. Graphite oxides were obtained by centrifuging it at 18,000 rpm for 30 min and washed it several times to remove the redundant H^+, and then pastes were stirred under vigorously ultrasonic conditions. GO was obtained by centrifugation and ultrasonication conditions. The morphology of GO was characterized by SEM (field emission scanning electron microscope, FEI-JSM 6320F) and TEM JEOL transmission electron microscope, JEM-2010, Japan). The XPS measurements were conducted with a Thermo ESCSLAB 250 electron spectrometer using 150 W Al Kα radiation. The surface functional groups of GO was recorded by using FT-IR spectroscopy measurements (Perkin-Elmer 100 spectrometer) in KBr pellet at room temperature.

2.3. Batch uptake experiments

The triple uptake experiments of Ni(II) on GO were conducted under N_2 conditions at $T = 293$ K in the presence of 0.01 mol/L NaCl. Briefly, the GO solution and NaCl were pre-equilibrated for 24 h, then Ni(II) stock solution were provided into the bulk suspension gradually in order to avoid generating $Ni(OH)_2$ precipitate. The pH values were adjusted to be in the range 2.0 to 11.0 by adding negligible volume of 0.1–1.0 mol/L $HClO_4$ or NaOH solution. Then suspensions were reacted under the stirring conditions for 48 h to ensure that the uptake reaction could achieve uptake equilibrium (preliminary experiments found that this was adequate for the suspension to obtain equilibrium). To eliminate the effect of Ni(II) uptake on tube walls, the uptake of Ni(II) without GO was carried out under the same experimental conditions. The solid phases were separated from liquid phases by centrifugation at 7000 rpm for 20 min, and then the supernatant was filtered by a 0.22-μm membrane. The concentration of Ni(II) in aqueous solutions was determined by atomic absorption spectroscopy (AAS-6300, Shimadzu). The amount of adsorbed Ni(II) was calculated by the difference in the initial and equilibrated concentration of Ni(II) in aqueous solutions.

2.4. Surface complexation modeling

The uptake of Ni(II) on GO at different pH and 0.01 mol/L NaCl conditions was fitted by using the diffuse layer model (DLM) with the aid of visual MINTEQL v 2.6 code [38]. The surface acidity constants ($\log K_1$ and $\log K_2$ values) were calculated as Eqs. (1) and (2):

$$SOH + H^+ = SOH_2^+ \quad (1)$$

$$SOH = SO^- + H^+ \quad (2)$$

where the values of $\log K_1$ and $\log K_2$ were obtained by fitting the data of acid-base titration at $I = 0.01$ mol/L NaCl solutions.

3. Results and discussion

3.1. Characterization

The morphology and microstructure of GO were characterized by SEM and TEM. As shown by SEM in Fig. 1A, GO was tightly accumulated together by randomly and thin nanosheets [39–41]. As shown in Fig. 1B, the average size of GO presented ~2.5 × 5.0 nm according to the high resolution TEM image [21]. Fig. 1C shows the deconvolution of high resolution O 1 s XPS spectra of GO. The major O 1 s peak of GO can be deconvoluted into three sub-peaks, including peaks at 531.55, 532.66 and 533.45 eV, which can be indexed into bridging –OH, –COO and adsorbed H_2O, respectively [21]. The results of XPS analysis indicated that GO presented a variety of oxygen-containing functional groups such as hydroxyl, epoxy, carboxyl and carbonyl groups. Fig. 1D shows the FT-IR spectrum of GO. The main bands at 1105, 1225, 1622 and 1725 cm^{-1} were ascribed to the C—H, C-OH, C═C and C═O group, respectively [42–44], indicating that GO displayed the large amounts of oxygen-containing functional groups such hydroxyl, carboxyl, epoxy and carbonyl groups. The N_2-BET specific surface area (SSA) of the as-prepared GO was 114 m^2/g, which was significantly lower than the theoretical value (~2700 m^2/g). It was assumed that the powder of GO could be easily aggregated together, which can result in the partial overlapping and coalescing of nanosheets [21].

3.2. Effect of reaction time

Fig. 2 shows the effect of contact time on Ni(II) uptake onto GO at pH 5.0 and $I = 0.01$ mol/L NaCl solutions. One can see that the uptake rate of Ni(II) on GO significantly enhanced with increasing reaction times within 3.0 h, then remained the high level uptake at reaction time > 6.0 h. At reaction time of 12 h, approximate 99.9% of Ni(II) was removed by GO, revealing that GO enhanced the rate and extent of Ni(II) uptake from aqueous solutions. The uptake data were fitted by pseudo-first-order kinetic and pseudo-second-order kinetic model. The equations of pseudo-first-order and pseudo-second-order kinetic models can be described by Eqs. (3) and (4), respectively:

$$\ln(q_e - q_t) = \ln q_e - k_f \times t \quad (3)$$

$$t/q_t = 1/(k_s \times q_e^2) + t/q_e \quad (4)$$

where q_e and q_t (mg/g) are the amount of Ni(II) adsorbed at equilibrium and at time t, respectively. k_f and k_s are the pseudo-first-order and pseudo-second-order kinetic rate constant, respectively. As summarized in Table 1, the maximum adsorption capacity obtained from pseudo-second-order kinetic model (9.874 mg/g) was more close to theoretical maximum adsorption capacity (12.5 mg/g) compared to the pseudo-first-order kinetic model (8.75 mg/g). The correlation coefficient ($R^2 = 1$) obtained from pseudo-second-order kinetic model was significantly higher than that of pseudo-first-order kinetic model ($R^2 < 0.67$). These evidences indicated that the uptake kinetics of Ni(II) on GO can be satisfactorily fitted be pseudo-second-order kinetic model, which was in accordance with previous studies [45–49].

3.3. pH and ionic strength effect

Fig. 3 shows the uptake of Ni(II) on GO as a function of pH in 0.001, 0.01 and 0.1 mol/L NaCl solutions. Approximate 30% of Ni(II) was uptake by GO at pH ~ 2.0, then Ni(II) uptake increased slightly with increasing pH starting from 2.0 to 6.0, and then kept the high level at pH > 6.0. Sun et al. demonstrated that the pH_{PZC} (pH at point of zero charge) of GO was calculated to be ~4.0 [36]. The distribution of Ni(II) in aqueous solutions was $Ni^{2+}/Ni(OH)^+$ and $Ni(OH)_2(aq)$ at pH < 9.5 and 9.5–11.0, respectively [50]. Therefore, the increased uptake of Ni(II) on GO at pH 2.0 and 6.0 could be attributed to the electrostatic attraction of negative charged of GO surface and positive charged of Ni(II) species (e.g., $Ni^{2+}/Ni(OH)^+$ species). The high level uptake of Ni(II) on GO could be due to the formation of surface co-precipitate such as $Ni(OH)_2(s)$.

The effect of ionic strength on the uptake of Ni(II) on GO was also showed in Fig. 3. As shown in Fig. 3, it is found that the uptake of Ni(II) on GO was independent of ionic strength. Previous studies demonstrated that the outer-sphere surface complexation was sensitive to

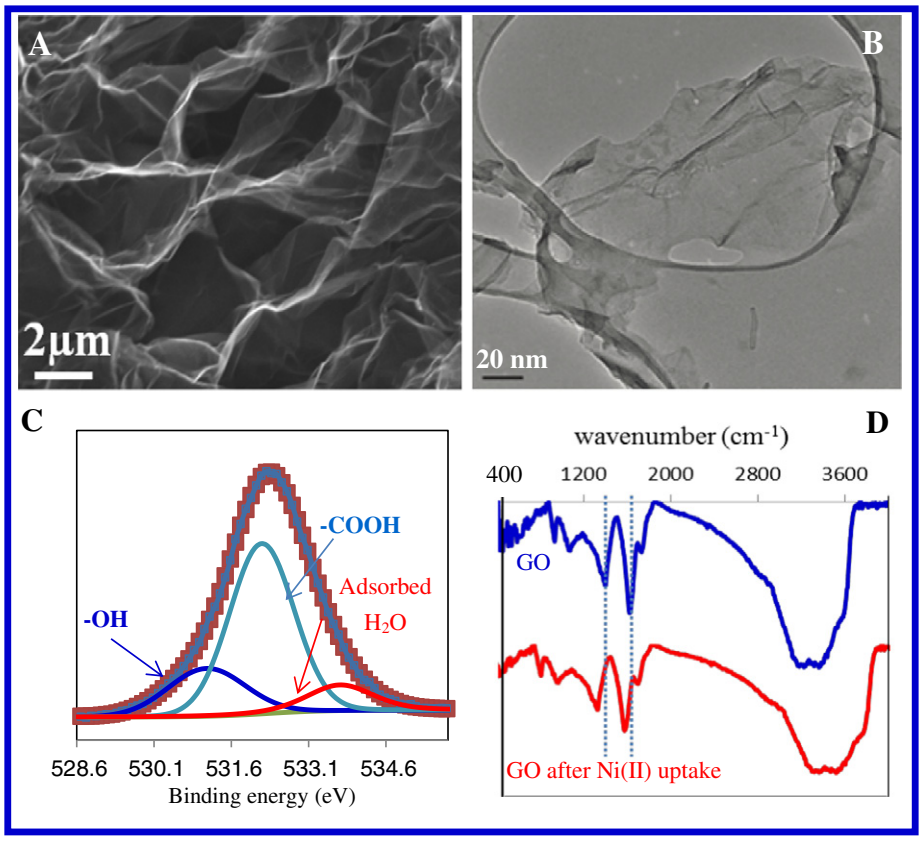

Fig. 1. Characterization of GO. A: SEM image; B: TEM image; C: XPS spectra; D: FT-IR spectrum.

the effect of ionic strength, whereas inner-sphere surface complexation was independent of ionic strength [51–53]. Therefore, the ionic strength-dependent experiments indicated that the uptake of Ni(II) on GO was inner- sphere surface complexation. The occurrence of plenty of surface oxygen functional groups on GO surface were favorable to form strong complexes with Ni(II) ions on the surfaces of GO.

3.4. Effect of Ni(II) concentration and temperature

Fig. 4 shows the uptake isotherms of Ni(II) on GO at pH 5.0 under $T = 293$, 323 and 333 K by batch technique. It is observed that the uptake of Ni(II) on GO significantly increased with increasing temperature. The uptake data of Ni(II) on GO were fitted by Langmuir and Freundlich models. The models of Langmuir and Frenudlich models can be expressed by Eqs. (5) and (6), respectively:

$$C_e/Q_e = 1/(q_{max} \times K_a) + C_e/q_{max} \quad (5)$$

$$Q_e = K_F \times C_e^{1/n} \quad (6)$$

where *Qe* (mg/g) and *Ce* (mg/L) are the amount of adsorbed Ni(II) on GO and equilibrium concentration in solution, respectively. q_{max} refers to the maximum adsorption capacity, and K_a(L/mg) and K_F —($mg^{1-n}g^{-1}L^n$) are the constants of Langmuir and Frenudlich model, respectively. 1/*n* refer to the Frenudlich exponent related to isotherm nonlinearity, respectively. The fitted parameters of Langmuir and Freundlich models were summarized in Table 2. As shown in Table 2, one can see that the uptake behaviors of Ni(II) on GO can be fitted by Langmuir model very well with high correlation coefficient ($R^2 > 0.995$) compared to Freundlich model ($R^2 < 0.985$). The maximum uptake capacity of Ni(II) on GO calculated from Langmuir model was 81.97 mg/g at pH 5.0 and 293 K. As shown by FT-IR spectrum of GO after Ni(II) uptake in Fig. 1D, the peaks of carboxyl (at ~1725 cm^{-1}) and hydroxyl (at ~1225 cm^{-1}) of GO were significantly lower than those of GO after Ni(II) uptake (at ~1730 and 1229 cm^{-1} for carboxyl and hydroxyl group, respectively), suggesting a covalent linkage of Ni(II) with carboxyl and hydroxyl groups [54]. Such high adsorption capacity of GO could be attributed to the abundant of

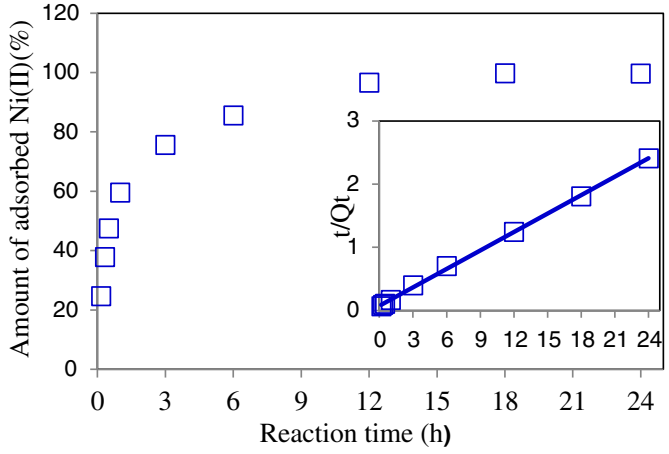

Fig. 2. Uptake kinetics of Ni(II) on GO, $C_0 = 10.0$ mg/L, pH 5.0, $I = 0.01$ mol/L NaCl, m/v = 0.8 g/L, $T = 293$ K.

Table 1
Parameters of pseudo-first-order and pseudo-second-order kinetic model for Ni(II) uptake by GO.

Pseudo-first-order				Pseudo-second-order		
q_e(mg/g)	k_f(h^{-1})	R^2	Q_{theo} (mg/g)	q_e(mg/g)	k_s(g/(mg × h))	R^2
8.75	0.003	0.652	12.5	9.874	0.00042	1

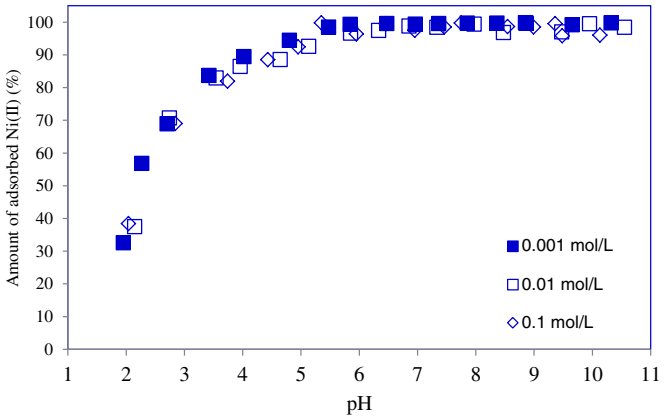

Fig. 3. Effect of ionic strength on the Ni(II) uptake on GO under different pH conditions, $C_0 = 10.0$ mg/L, m/v = 0.8 g/L, $T = 293$ K.

various oxygenated function groups such as hydroxyl, epoxy and carboxyl groups.

The thermodynamic parameters (Gibbs free energy change-ΔG^0, enthalpy change-ΔH^0 and entropy change-ΔS^0) of uptake of Ni(II) on GO can be calculated from the temperature dependent uptake isotherms. The values of ΔG^0 can be calculated by Eq. (7):

$$\Delta G^0 = -RT \ln K_d{}^0 \quad (7)$$

where R and T are the ideal gas constant (8.314 J/(mol·K)) and temperature in Kelvin, respectively. The values of ΔH^0 and ΔS^0 can be calculated from the slope and intercept of the plot of ln K_d^0 vs. 1/T:

$$\ln K_d{}^0 = \Delta S^0/R - \Delta H^0/RT \quad (8)$$

These parameters were summarized in Table 3. As shown in Table 3, the negative ΔG^0 values (e.g., −25.48 and −30.33 kJ/mol at 293 and 333 K, respectively) indicated that the uptake of Ni(II) on GO was a favorably spontaneous process [55]. The decrease of ΔG^0 with increasing temperatures revealed that the uptake of Ni(II) on GO was more favorable at higher temperature. The positive ΔH^0 value (10.12 kJ/mol) indicated that Ni(II) uptake by GO was an endothermic process. Previous studies determined that the dehydration of Ni(II) from aqueous Ni(II) complex ion was an endothermic process, but attachment of Ni(II) to the surface of GO was an exothermic process [56–63]. It is plausible to assume that the energy of dehydration exceeded the exothermicity of the Ni(II) ions attached to the surface of GO. The positive value of ΔS^0 (121.55 J/(mol·K)) also demonstrated that the Ni(II) uptake by GO was a spontaneous process [64].

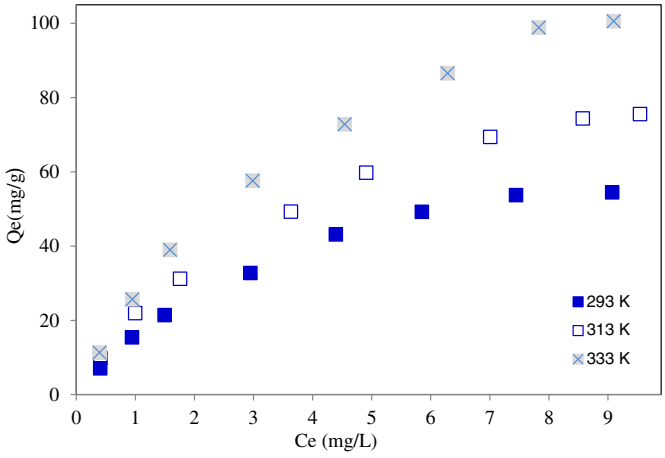

Fig. 4. Uptake isotherms of Ni(II) on GO under different temperature, $C_0 = 10.0$ mg/L, pH 5.0, $I = 0.01$ mol/L NaCl, m/v = 0.8 g/L.

Table 2
Parameters of Langmuir and Freundlich model for Ni(II) uptake by GO.

	Langmuir			Freundlich		
	K_a	q_{max} (L/mg)	R^2 (mg/g)	ln K_F (mg/g)/(mg/g)^n	1/n	R^2
293 K	0.240	81.97	0.994	2.705	0.6577	0.979
323 K	0.238	109.9	0.997	3.003	0.6360	0.983
333 K	0.201	156.3	0.995	3.215	0.6849	0.983

Table 3
Thermodynamic parameters for Ni(II) uptake by GO.

Temperature	ΔG^0(kJ/mol)	ΔH^0(kJ/mol)	ΔS^0(J/(mol·K))
293 K	−25.48		
323 K	−27.97	10.12	121.55
333 K	−30.33		

3.5. Surface complexation modeling

According to the ionic strength-dependent adsorption experiments, two main uptake reactions were accounted into Eqs. (9) and (10):

$$SOH + Ni^{2+} = SONi^{+} + H^{+} \quad (9)$$

$$SOH + Ni^{2+} + 2H_2O = SONi(OH)_2^{-} + 3H^{+} \quad (10)$$

where SOH represents a structurally undefined, average functional group (assumed to be an amphoteric hydroxyl group) on the surface of GO. The log K values were optimized by best fitting of the uptake of Ni(II) on GO (Table 4). As shown in Fig. 5, DLM can give better fit for the uptake data of Ni(II) on GO. Clearly, the two reactions were sufficient to depict Ni(II) uptake on GO in the pH range from 2.0 to 10.0. As shown in Fig. 5, one can see that the main Ni(II) species was $SONi^+$ species at pH < 5.0, whereas $SONi(OH)_2^-$ species dominated the uptake of Ni(II) on GO at pH > 5.0. The results of surface complexation modeling indicated that the uptake of Ni(II) on GO can be satisfactorily fitted by DLM model with two inner-sphere surface complexes ($SONi^+$ and $SONi(OH)_2^-$ species), which was consistent with previous studies [65]. These findings indicated that the uptake mechanism of Ni(II) on GO was inner-sphere surface complexation over wide pH range starting from 2.0 to 10.0.

4. Conclusions

The uptake reactions at the water-solid interface generally decrease solute mobility and often control the fate, bioavailability, and transport of Ni(II) in soils and groundwater. In this study, uptake of Ni(II) ions on GO has been systematically investigated as a function of several environmental factors including reaction time, pH, ionic strength, concentration and temperature. The pseudo-second-order kinetic model and Langmuir model given better fits to the uptake kinetics and uptake

Table 4
The optimized parameters for surface complexation modeling of Ni(II) uptake by GO.

Equations	Log K
$SOH + H^+ = SOH_2^+$	4.22
$SOH = SO^- + H^+$	−5.31
$SOH + Ni^{2+} = SONi^+ + H^+$	2.18
$SOH + Ni^{2+} + 2H_2O = SONi(OH)_2^- + 3H^+$	−3.42

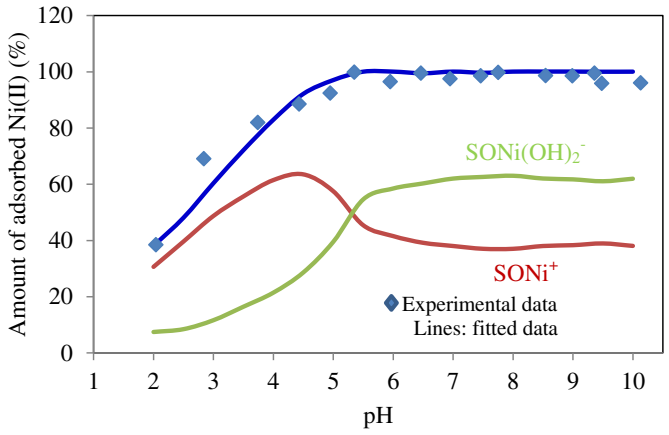

Fig. 5. Surface complexation modeling of Ni(II) uptake on GO under different pH condition, $C_0 = 10.0$ mg/L, $I = 0.01$ mol/L NaCl, m/v = 0.8 g/L, $T = 293$ K.

isotherms of Ni(II) on GO, respectively. The maximum uptake capacity of GO for Ni(II) calculated from Langmuir model was calculated to be 81.97 mg/g at pH 5.0 and 293 K. The data obtained from isothermal uptake at different temperature indicated that the uptake of Ni(II) on GO was an exothermal and spontaneous process. The uptake mechanism of Ni(II) on GO were demonstrated by XPS analysis and surface complexation modeling. The highly effective uptake of Ni(II) was attributed to oxygen-containing functional groups of GO according to XPS analysis. The surface complexation modeling indicated that the uptake of Ni(II) on GO can be satisfactorily fitted by diffuse layer model with two inner-sphere complexes ($SONi^+$ and $SONi(OH)_2^-$ species). These results indicated that GO can be used as a promising adsorbent for the uptake of heavy metals from aqueous solutions in environmental remediation strategies.

Acknowledgements

Financial support from National Natural Science Foundation of China (31601268), Apple Orchards Marsh Fertilizer Application Technology Research and Demonstration Project of Agriculture Ministry (K312021012), Agricultural Special Fund Project of Shaanxi Province (K332021312) are acknowledged.

References

[1] T.A. Kurniawan, G.Y.S. Chan, W.H. Lo, S. Babel, Physico-chemical treatment techniques for wastewater laden with heavy metals, Chem. Eng. J. 118 (2006) 83–98.
[2] D.C. Adriano, Trace Elements in the Terrestrial Environment, Springer, Berlin, 1986 362–389.
[3] S.B. Yang, C.C. Ding, W.C. Cheng, Z.X. Jin, Y.B. Sun, Effect of microbes on Ni(II) diffusion onto sepiolite, J. Mol. Liq. 204 (2015) 170–175.
[4] R.G. Ford, A.C. Scheinost, K.G. Scheckel, D.L. Sparks, The link between clay mineral weathering and the stabilization of Ni surface precipitates, Environ. Sci. Technol. 33 (1999) 3140–3144.
[5] H. Marcussen, P.E. Holm, B.W. Strobel, H.C.B. Hansen, Nickel sorption to goethite and montmorillonite in presence of citrate, Environ. Sci. Technol. 43 (2009) 1122–1127.
[6] M.H. Bradbury, B. Baeyens, Experimental measurements and modeling of sorption competition on montmorillonite, Geochim. Cosmochim. Acta 69 (2005) 4187–4197.
[7] M.H. Bradbury, B. Baeyens, Modelling the sorption of Mn(II), Co(II), Ni(II), Zn(II), Cd(II), Eu(III), Am(III), Sn(IV), Th(IV), Np(V) and U(VI) on montmorillonite: linear free energy relationships and estimates of surface binding constants for some selected heavy metals and actinides, Geochim. Cosmochim. Acta 69 (2005) 875–892.
[8] R. Dahn, A.M. Scheidegger, A. Manceau, M.L. Schlegel, B. Baeyens, M.H. Bradbury, D. Chateigner, Structural evidence for the sorption of Ni(II) atoms on the edges of montmorillonite clay minerals: a polarized X-ray absorption fine structure study, Geochim. Cosmochim. Acta 67 (2003) 1–15.
[9] X. Gu, L.J. Evans, Surface complexation modelling of Cd(II), Cu(II), Ni(II), Pb(II) and Zn(II) adsorption onto kaolinite, Geochim. Cosmochim. Acta 72 (2008) 267–276.
[10] S. Yang, X. Ren, G. Zhao, W. Shi, G. Montavon, B. Grambow, X. Wang, Competitive sorption and selective sequence of Cu(II) and Ni(II) on montmorillonite: batch, modeling, EPR and XAS studies, Geochim. Cosmochim. Acta 166 (2015) 129–145.
[11] M.H. Ma, H.Y. Gao, Y.B. Sun, M.S. Huang, The adsorption and desorption of Ni(II) on Al substituted goethite, J. Mol. Liq. 201 (2015) 30–35.
[12] Y. Arai, Spectroscopic evidence for Ni(II) surface speciation at the iron oxyhydroxides-water interface, Environ. Sci. Technol. 42 (2008) 1151–1156.
[13] G. Montavon, E. Alhajji, B. Grambow, Study of the interaction of Ni^{2+} and Cs^+ on MX-80 bentonite; effect of compaction using the "capillary method", Environ. Sci. Technol. 40 (2006) 4672–4679.
[14] A.M. Scheidegger, G.M. Lamble, D.L. Sparks, Investigation of Ni sorption on pyrophyllite: an XAFS study, Environ. Sci. Technol. 30 (1996) 548–554.
[15] T.J. Strathmann, S.C.B. Myneni, Effect of soil fulvic acid on nickel(II) sorption and bonding at the aqueous-boehmite (gamma-AlOOH) interface, Environ. Sci. Technol. 39 (2005) 4027–4034.
[16] P. Trivedi, L. Axe, T.A. Tyson, XAS studies of Ni and Zn sorbed to hydrous manganese oxide, Environ. Sci. Technol. 35 (2001) 4515–4521.
[17] L.P. Lingamdinne, J.R. Koduru, Y.L. Choi, Y.Y. Chang, J.K. Yang, Studies on removal of Pb(II) and Cr(III) using graphene oxide based inverse spinel nickel ferrite nanocomposite as sorbent, Hydrometallurgy 65 (2016) 64–72.
[18] X. Wang, Y. Pei, M. Lu, X. Lu, X. Du, Highly efficient adsorption of heavy metals from wastewaters by graphene oxide-ordered mesoporous silica metarials, J. Mater. Sci. 50 (2015) 2113–2121.
[19] X.Y. Li, H.H. Zhou, W.Q. Wu, S.D. Wei, Y. Xu, Y.F. Kuang, Studies of heavy metals adsorption on chistosan/sulfydryl-functionalized graphene oxide composites, J. Colloid Interface Sci. 448 (2015) 389–397.
[20] Y. Yuan, G.H. Zhang, L. Li, G.L. Zhang, F.B. Zhang, X.B. Fan, Poly(amidoamine) modified graphene oxide as an efficient adsorbent for heavy metal ions, Polym. Chem. 4 (2013) 216402167.
[21] Z. Huang, X. Zheng, W. Lv, M. Wang, Q. Yang, F. Kang, Adsorption of lead(II) ions from aqueous solution on low-temperature exfoliated graphene nanosheets, Langmuir 27 (2011) 7558–7562.
[22] L.P. Lingamdinne, J.R. Koduru, H. Roh, Y.L. Choi, Y.Y. Chang, J.K. Yang, Adsorption removal of Co(II) from waste-water using graphene oxide, Hydrometallurgy 165 (2016) 90–96.
[23] A. Gopalakrishnan, R. Krishnan, S. Thangavel, G. Venugopal, S.J. Kim, Removal of heavy metal ions from pharma-effluents using graphene-oxide nanosorbents and study of their adsorption kinetics, J. Ind. Eng. Chem. 30 (2015) 14–19.
[24] L.P. Lingamdinne, Y.L. Choi, I.S. Kim, Y.Y. Chang, J.R. Koduru, J.K. Yang, Porous graphene oxide based inverse spinel nickel ferrite nanocomposites for the enhanced adsorption removal of arsenic, RSC Adv. (2016) 73776–73789.
[25] G. Zhao, J. Li, X. Ren, C. Chen, X. Wang, Few-layered grapheme oxide nanosheets as superior sorbents for heavy metal ion pollution management, Environ. Sci. Technol. 45 (2011) 10454–10462.
[26] C.C. Ding, W.C. Cheng, X.X. Wang, Z.-Y. Wu, Y.B. Sun, X.K. Wang, S.-H. Yu, Competitive sorption of Pb(II), Cu(II) and Ni(II) on carbonaceous nanofibers: a spectroscopic and modeling approach, J. Hazard. Mater. 313 (2016) 253–261.
[27] X. Guo, B. Du, Q. Wei, J. Yang, L. Hu, L. Yan, W. Xu, Synthesis of amino functionalized magnetic graphenes composite material and its application to remove Cr(VI), Pb(II), Hg(II), Cd(II) and Ni(II) from contaminated water, J. Hazard. Mater. 278 (2014) 211–220.
[28] P. Tan, J. Sun, Y. Hu, Z. Fang, Q. Bi, Y. Chen, J. Cheng, Adsorption of Cu^{2+}, Cd^{2+} and Ni^{2+} from aqueous single metal solutions on graphene oxide membranes, J. Hazard. Mater. 297 (2015) 251–260.
[29] X. Li, F. Li, L. Fang, Effect of *Paecilomyces cateniannulatus* on the adsorption of nickel onto graphene oxide, Korean J. Chem. Eng. 32 (2015) 2449–2455.
[30] B. Zawisza, A. Baranik, E. Malicka, E. Talik, R. Sitko, Preconcentration of Fe(III), Co(II), Ni(II), Cu(II), Zn(II) and Pb(II) with ethylenediamine-modified graphene oxide, Microchim. Acta 183 (2016) 231–240.
[31] E.C. Salihi, J. Wang, D.J.L. Coleman, L. Siller, Enhanced removal of nickel(II) ions from aqueous solutions by SDS-functionalized graphene oxide, Sep. Sci. Technol. 51 (2016) 1317–1327.
[32] J.Y. Huang, Z.W. Wu, L.W. Chen, Y.B. Sun, The sorption of Cd(II) and U(VI) on sepiolite: a combined experimental and modeling studies, J. Mol. Liq. 209 (2015) 706–712.
[33] Y.B. Sun, X.X. Wang, W.C. Song, S.H. Lu, C.L. Chen, X.K. Wang, Mechanistic insights on the decontamination of Th(IV) on graphene oxide-based composites by EXAFS and modeling techniques, Environ. Sci. Nano (2017)http://dx.doi.org/10.1039/C1036EN00470A.
[34] J.Y. Huang, Z.W. Wu, L.W. Chen, Y.B. Sun, Surface complexation modeling of adsorption of Cd(II) on graphene oxides, J. Mol. Liq. 209 (2015) 753–758.
[35] Y.B. Sun, Z.-Y. Wu, X.X. Wang, C.C. Ding, W.C. Cheng, S.-H. Yu, X.K. Wang, Macroscopic and microscopic investigation of U(VI) and Eu(III) adsorption on carbonaceous nanofibers, Environ. Sci. Technol. 50 (2016) 4459–4467.
[36] Y.B. Sun, Q. Wang, C.L. Chen, X.L. Tan, X.K. Wang, Interaction between Eu(III) and graphene oxide nanosheets investigated by batch and extended X-ray absorption fine structure spectroscopy and by modeling techniques, Environ. Sci. Technol. 46 (2012) 6020–6027.
[37] W.S. Hummers, R.E. Offeman, Preparation of graphitic oxide, J. Am. Chem. Soc. 80 (1958) 1339.
[38] J.P. Gustafsson, A windows version of MINTEQ, http://www.lwr.kth.se/English/OurSOrware/vminteq/index.htm2009.
[39] Y.B. Sun, S.B. Yang, G.X. Zhao, Q. Wang, X.K. Wang, Adsorption of polycyclic aromatic hydrocarbons on graphene oxides and reduced graphene oxides, Chem. Asian. J. 8 (2013) 2755–2761.
[40] Z.X. Jin, X.X. Wang, Y.B. Sun, Y.J. Ai, X.K. Wang, Adsorption of 4-n-nonylphenol and bisphenol-A on magnetic reduced graphene oxides: a combined experimental and theoretical studies, Environ. Sci. Technol. 49 (2015) 9168–9175.
[41] W.C. Cheng, M.L. Wang, Z.G. Yang, Y.B. Sun, C.C. Ding, The efficient enrichment of U(VI) by graphene oxide-supported chitosan, RSC Adv. 4 (2014) 61919–61926.
[42] C.C. Ding, W.C. Cheng, Y.B. Sun, X.K. Wang, Novel fungus-Fe_3O_4 bio-nanocomposites as high performance adsorbents for the removal of radionuclides, J. Hazard. Mater. 295 (2015) 127–137.

[43] W.C. Cheng, C.C. Ding, X.X. Wang, Z.-Y. Wu, Y.B. Sun, S.-H. Yu, T. Hayat, X.K. Wang, Competitive sorption of As(V) and Cr(VI) on carbonaceous nanofibers, Chem. Eng. J. 293 (2016) 311–318.
[44] Y.B. Sun, C.L. Chen, D.D. Shao, J.X. Li, X.L. Tan, G.X. Zhao, S.B. Yang, X.K. Wang, Enhanced adsorption of ionizable aromatic compounds on humic acid-coated carbonaceous adsorbents, RSC Adv. 2 (2012) 10359–10364.
[45] S.T. Yang, D.L. Zhao, G.D. Sheng, Z.Q. Guo, Y.B. Sun, Investigation of solution chemistry effects on sorption behavior of radionuclide Cu-64(II) on illite, J. Radioanal. Nucl. Chem. 289 (2011) 467–477.
[46] Y.B. Sun, S.T. Yang, G.D. Sheng, Z.Q. Guo, X.L. Tan, J.Z. Xu, X.K. Wang, Comparison of U(VI) removal from contaminated groundwater by nanoporous alumina and non-nanoporous alumina, Sep. Purif. Technol. 83 (2011) 196–203.
[47] W.C. Cheng, C.C. Ding, Y.B. Sun, M.L. Wang, The sequestration of U(VI) on functional beta-cyclodextrin-attapulgite nanorods, J. Radioanal. Nucl. Chem. 302 (2014) 385–391.
[48] Y.B. Sun, S.T. Yang, G.D. Sheng, Z.Q. Guo, X.K. Wang, The removal of U(VI) from aqueous solution by oxidized multiwalled carbon nanotubes, J. Environ. Radioact. 105 (2012) 40–47.
[49] C.C. Ding, W.C. Cheng, Z.X. Jin, Y.B. Sun, Plasma synthesis of beta-cyclodextrin/$Al(OH)_3$ composites as adsorbents for removal of UO_2^{2+} from aqueous solutions, J. Mol. Liq. 207 (2015) 224–230.
[50] G.D. Sheng, S.T. Yang, J. Sheng, D.L. Zhao, X.K. Wang, Influence of solution chemistry on the removal of Ni(II) from aqueous solution to titanate nanotubes, Chem. Eng. J. 168 (2011) 178–182.
[51] Y.B. Sun, S.B. Yang, Q. Wang, A. Alsaedi, X.K. Wang, Sequestration of uranium on fabricated aluminum co-precipitated with goethite (Al-FeOOH), Radiochim. Acta 102 (2014) 797–804.
[52] Y.B. Sun, R. Zhang, C.C. Ding, X.X. Wang, W.C. Cheng, C.L. Chen, X.K. Wang, Adsorption of U(VI) on sericite in the presence of *Bacillus subtilis*: a combined batch, EXAFS and modeling techniques, Geochim. Cosmochim. Acta 180 (2016) 51–65.
[53] W.C. Cheng, C.C. Ding, Y.B. Sun, X.K. Wang, Fabrication of fungus/attapulgite composites and their removal of U(VI) from aqueous solution, Chem. Eng. J. 269 (2015) 1–8.
[54] Y.B. Sun, D.D. Shao, C.L. Chen, S.B. Yang, X.K. Wang, Highly efficient enrichment of radionuclides on graphene oxide-supported polyaniline, Environ. Sci. Technol. 47 (2013) 9904–9910.
[55] Q. Wang, L. Chen, Y.B. Sun, Removal of radiocobalt from aqueous solution by oxidized MWCNT, J. Radioanal. Nucl. Chem. 291 (2012) 787–795.
[56] Y.B. Sun, S.B. Yang, C.C. Ding, Z.X. Jin, W.C. Cheng, Tuning the chemistry of graphene oxides by a sonochemical approach: application of adsorption properties, RSC Adv. 5 (2015) 24886–24892.
[57] X.X. Wang, Q.H. Fan, S.J. Yu, Z.S. Chen, Y.J. Ai, Y.B. Sun, A. Hobiny, A. Alsaedi, X.K. Wang, High sorption of U(VI) on graphene oxides studied by batch experimental and theoretical calculations, Chem. Eng. J. 287 (2016) 448–455.
[58] Y.B. Sun, S.B. Yang, Y. Chen, C.C. Ding, W.C. Cheng, X.K. Wang, Adsorption and desorption of U(VI) on functionalized graphene oxides: a combined experimental and theoretical study, Environ. Sci. Technol. 49 (2015) 4255–4262.
[59] C.C. Ding, W.C. Cheng, Y.B. Sun, X.K. Wang, Determination of chemical affinity of graphene oxide nanosheets with radionuclides investigated by macroscopic, spectroscopic and modeling techniques, Dalton Trans. 43 (2014) 3888–3896.
[60] W.C. Song, T.T. Yang, X.X. Wang, Y.B. Sun, Y.J. Ai, G.D. Sheng, T. Hayat, X.K. Wang, Experimental and theoretical evidence for competitive interactions of tetracycline and sulfamethazine with reduced graphene oxides, Environ. Sci. Nano 3 (2016) 1318–1326.
[61] Y.B. Sun, C.C. Ding, W.C. Cheng, X.K. Wang, Simultaneous adsorption and reduction of U(VI) on reduced graphene oxide-supported nanoscale zerovalent iron, J. Hazard. Mater. 280 (2014) 399–408.
[62] Z.X. Jin, J. Sheng, Y.B. Sun, Characterization of radioactive cobalt on graphene oxide by macroscopic and spectroscopic techniques, J. Radioanal. Nucl. Chem. 299 (2014) 1979–1986.
[63] Y.B. Sun, X.X. Wang, C.C. Ding, W.C. Cheng, C.L. Chen, T. Hayat, A. Alsaedi, J. Hu, X.K. Wang, Direct synthesis of bacteria-derived carbonceous nanofibers as a highly efficient material for radionuclides elimination, ACS Sustain. Chem. Eng. 4 (2016) 4608–4616.
[64] C.C. Ding, W.C. Cheng, Y.B. Sun, X.K. Wang, Effects of *Bacillus subtilis* on the reduction of U(VI) by nano-Fe^0, Geochim. Cosmochim. Acta 165 (2015) 86–107.
[65] Y.B. Sun, J.X. Li, X.K. Wang, The retention of uranium and europium onto sepiolite investigated by macroscopic, spectroscopic and modeling techniques, Geochim. Cosmochim. Acta 140 (2014) 621–643.